Textures and Microstructures, 1991, Vol. 13, pp. 189–197
Reprints available directly from the publisher.
Photocopying permitted by license only

RESOLUTION OF SUPERIMPOSED DIFFRACTION PEAKS IN TEXTURE ANALYSIS OF A $YBa_2Cu_3O_7$ POLYCRYSTAL

JOHN S. KALLEND,[1] R. B. SCHWARZ[2] and A. D. ROLLETT[2]

[1]*Department of Metallurgical and Materials Engineering, Illinois Institute of Technology, Chicago, IL 60616, USA*
[2]*Center for Materials Science, Los Alamos National Laboratory, K-765, Los Alamos, NM 87545, USA*

(Received September 1 1990; in final form November 3, 1990)

Texture measurements in polycrystalline 123 oxide superconductors are complicated by the superposition of Bragg reflections in the pole figures due to the near degeneracy of the crystal structure. A method is described, based on an extension of the WIMV algorithm, for resolving these superpositions and determining the crystal orientation distribution (OD). The method is exemplified by OD analysis of a magnetically aligned, strongly textured powder sample of $YBa_2Cu_3O_7$.

KEY WORDS ODF analysis, WIMV method, superposed peaks, $YBa_2Cu_3O_7$, magnetic alignment.

1. INTRODUCTION

In single crystals and epitaxially grown thin films of $YBa_2Cu_3O_7$, the superconducting critical current density, J_c, at 77 K and zero magnetic field is in the range 10^5–10^6 A cm^{-2}, whereas in bulk polycrystalline samples lacking preferred texture, J_c rarely exceeds 10^3 A cm^{-2}. This large difference in J_c suggests that the random arrangement of grains, and possibly intrinsic properties of the grain boundaries, limit J_c. To improve the transport current characteristics, researchers have prepared textured polycrystalline samples. For example, Jin and co-workers (1988) measured J_c of 17,000 A cm^{-2} in bulk samples prepared by directional solidification whereas Salama *et al.* (1989) used a liquid phase processing technique to achieve J_c in excess of 18,500 A cm^{-2}. In none of these measurements was the texture of the samples characterized quantitatively. An example in which the texture/property relationship is unambiguous, however, is as follows. In two thick films of the Y-123 compound that were made by electrophoretic deposition, (Hein *et al.*, 1989) the surface resistivity was found to be significantly different. Measurements of pole figures for these films (Rollett, 1989) showed a fiber texture with a degree of ⟨001⟩ alignment perpendicular to the film plane that was significantly higher in the film that had the better properties. The improvement in crystallographic alignment was the result of using a magnetic field to align the particles during the deposition process.

Three independent parameters (e.g. three Euler angles in a given reference frame) are required to describe the orientation of a three dimensional object, such as a crystal lattice. A complete description of the texture of any polycrystalline sample is provided by the three-dimensional orientation distribution (OD), (Kocks, 1988). This describes the distribution of crystal lattice orientations as a function of the three Euler angles. Direct determination of the OD is not possible, but it may be inferred from a finite number of pole figure measurements, each describing the distribution of certain crystal directions (the poles of diffracting planes) over the surface of a sphere. The pole figure data is two dimensional, and represents the projection of the OD onto the unit sphere along a path which depends on the orientation of the diffracting vector. Reconstruction of the OD from pole figures is, therefore, similar to the familiar problem of tomographic reconstruction.

X-ray pole figure goniometers are designed to measure the diffracted intensity from a sample as it is tilted and rotated to different orientations with respect to the X-ray beam. Severe defocussing of the diffracted beam occurs at high angles of tilt, which necessitates operation with much wider slits at the detector than is customary in normal powder diffraction. The combination of defocussing and the use of wide slits severely limits the resolution of the diffracting angle contributing to the pole figure. This limits the accuracy of texture analysis in polycrystalline samples having closely spaced Bragg reflections. Such is the case in the orthorhombic 123 superconducting oxides; because in these the degree of orthorhombicity is low ($b/a \approx 1.03$) and $c/a \approx 3$, many of the Bragg peaks are very closely spaced or even superimpose. The limited angular resolving power of the pole figure goniometer means that pole figures measured from such peaks are inevitably the superposition of the pole figures due to the individual forms. This makes pole figure interpretation and the task of OD reconstruction from the pole figures much more complicated. In fact, these difficulties have prompted the use of less satisfactory texture measuring procedures, such as the use of rocking curves and "inverse pole figures" measured with a normal powder diffractometer.

Several methods are available for the determination of ODs from pole figures. The most widespread uses spherical harmonic analysis of the data (Bunge, 1965 and Roe, 1965) but requires a large number of independent pole figures in order to achieve a satisfactory solution for crystals of low symmetry (e.g. 12 pole figures for a solution to $l = 22$ in orthorhombic crystals). It also becomes more complex if incomplete pole figures are used, as in the normal Schultz reflection geometry. However, the analysis of superposed peaks by this method is possible by a deconvolution procedure based on relative intensity differences (Baker and Wenk, 1972, also Bunge, 1982).

The Williams–Imhof–Matthies–Vinel (WIMV) algorithm (Matthies and Vinel, 1982) is an iterative procedure leading to a maximum entropy solution for the OD. It results in a smooth topology with a minimum number of strong peaks, while providing a best fit to the experimental data. We have elected to use this algorithm because it is more economical in its requirements for pole figure data than the harmonic method, a feature that makes it well suited for the analysis of low-symmetry crystals and incomplete pole figures. However, modification is necessary to handle pole figures from superposed diffraction peaks.

WIMV requires the projection geometry between the OD and the pole figures to be established. Our implementation divides the OD space into a $5 \times 5 \times 5$

degree grid in the three Euler angles, and the pole figures into a 5×5 degree polar grid. A set of pointers is used to relate each OD cell with its corresponding pole figure cell. The first estimate of the value in an OD cell is made by taking the geometric mean of the values in the corresponding pole figure cells. This estimated OD is used to calculate the pole figures that it would produce using the projection geometry established as described above. These calculated pole figures will not, in general, correspond very well with the actual measurements. The ratios of the actual to calculated values are used to calculate a correction factor which is used to improve the OD estimate. This procedure converges rapidly, and typically 6 to 12 iterations will produce a satisfactory solution when good quality pole figures are available.

We have modified the WIMV algorithm to handle superposed pole figures using relative intensity differences from the different forms to achieve the separation. The details are described elsewhere (Kallend *et al.*, 1990) and will only be presented in outline here. The set of pointers used to establish the projection geometry between the OD and the pole figures is now associated with the relative weight assigned to each form contributing to the pole figure. The weights are simply determined from the calculated relative intensities of their reflections. The remainder of the algorithm is essentially as before, except that weighted values are now used in making the original OD estimate, recalculating the pole figures, and evaluating the correction factors. The accuracy of the final result depends primarily on the accuracy of the pole figure recalculations from the successive estimations of the OD. The OD is refined until it produces recalculated pole figures that agree with the experimental data to the desired degree of accuracy. Fortunately this step is precisely defined if the unit cell geometry and the relative intensities are known. We have found, however, that faster convergence occurs if the other steps (calculation of the original estimate and of correction factors) use the square of the relative intensities as weighting factors.

The speed of convergence of this procedure depends sensitively on the nature of the available data and the relative intensity differences for superposed poles. In particular, if two superposed poles have identical relative intensities, and no other data are available in the pole figure set to arbitrate, no unique OD solution will be available since a whole spectrum of possible solutions will fit the measurements equally well. On the other hand, rapid separation of superposed peaks occurs if the relative intensities are significantly different, or if the information content of another pole figure is able to resolve the superposition.

2. APPLICATION TO A MAGNETICALLY ALIGNED 123 SUPERCONDUCTOR

A sample of $YBa_2Cu_3O_7$ powder having a high degree of texture was prepared by casting the powder in epoxy cement while aligning the particles in a magnetic field. The $YBa_2Cu_3O_7$ powder was made by the standard solid-state reaction of oxide and carbonates. Particles with diameters less than 20 μm were separated by sifting. These small particles are more likely to be single crystals and thus have a larger probability of becoming oriented in the liquid epoxy under the influence of the applied magnetic field. The powder was mixed with Stycast 1266

two-part epoxy (Emerson and Cuming) which was cured in a solenoidal magnetic field of 4.2 T. Cylindrical samples were cut from the cured epoxy with the cut surface parallel to the applied magnetic field. Reflection pole figures were measured to a tilt angle of 80 degrees using Cu–Kα radiation with a Huber pole figure goniometer. The measured pole figures are shown in Figure 1. Figure 1a is

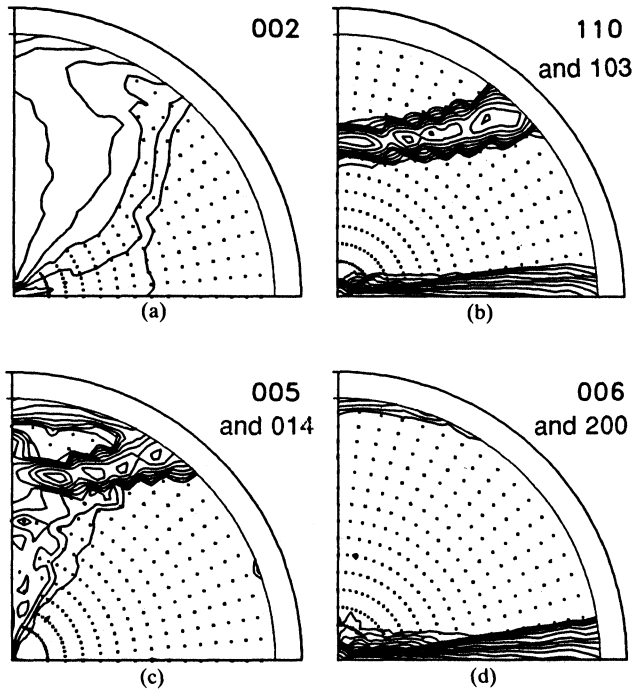

Figure 1 (a) Measured {002} pole figure from $YBa_2Cu_3O_7$ powder magnetically aligned in epoxy. In all the figures, the contours are labeled in the side-bar as multiples of a random intensity. (b) Measured {110} pole figure with superimposed {103} pole figure. (c) Measured {005} pole figure with superimposed {014} pole figure. (d) Measured {006} pole figure with superimposed {200} pole figure. In this and subsequent figures, there are ten contours, logarithmically spaced, and the regions that have intensity below the random level (= 1) are dotted at 5° intervals.

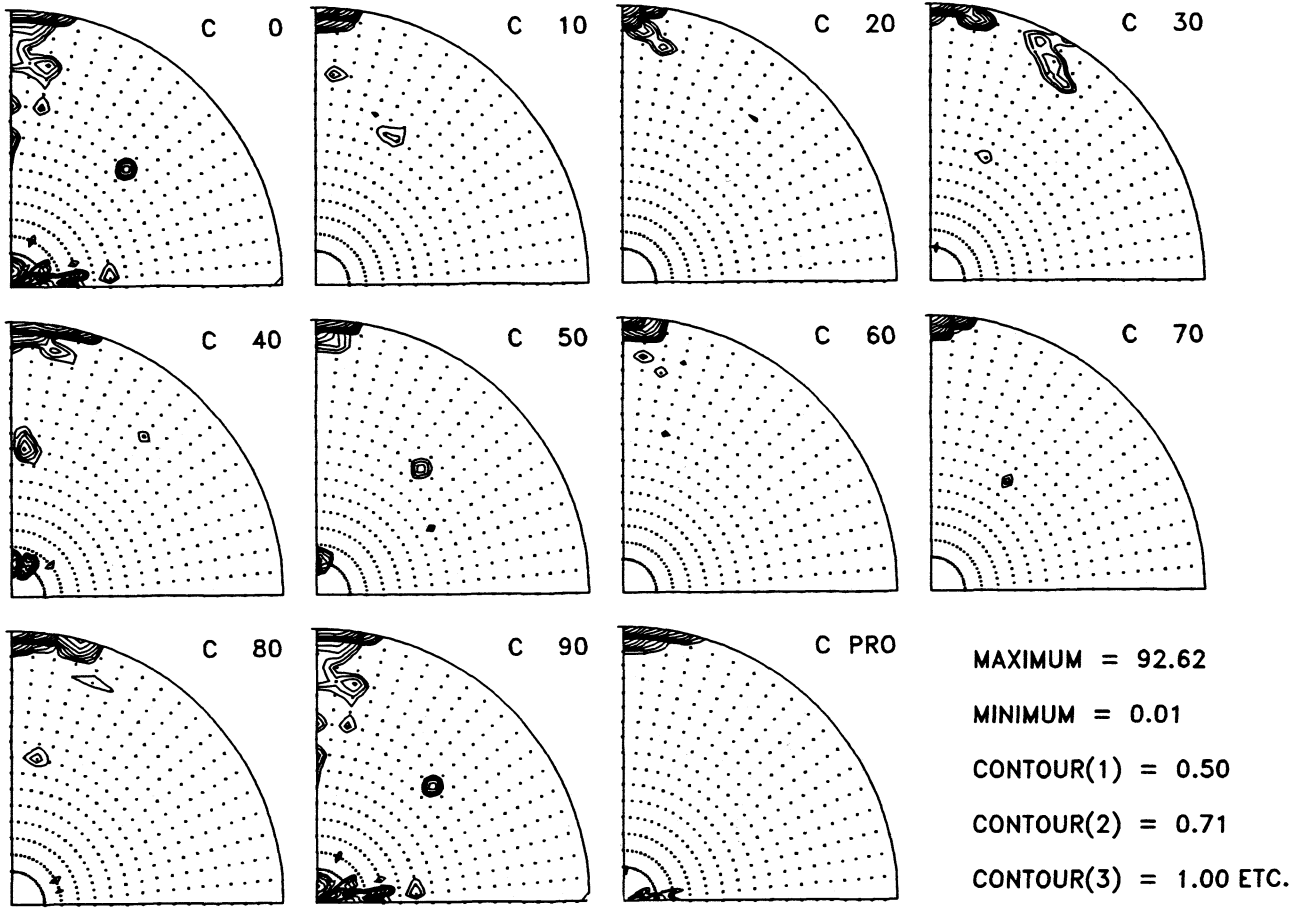

Figure 2 Orientation Distribution calculated from pole figures shown in Figure 1. The OD is displayed as sections at constant ν with ψ on the azimuth. The last quadrant (C PRO) is the mean of the sections and shows the inverse pole figure for the sample. The sections show that the texture of the sample is an $\langle 001 \rangle$ fiber lying in the plane of the sample.

the {002} pole figure, Figure 1b is from the superposed {103} and {110}, Figure 1c is from the superposed {005} and {014}, and Figure 1d from the superposed {006} and {200} reflections. The magnetic field direction projects towards the top of these pole figures, i.e. it is parallel to the 1 direction. Examination of the diffraction data indicates that there is no information in these figures that could allow a separation of the *a* and *b* axes of the orthorhombic structure and so the data were analyzed as if the crystal structure were tetragonal.

Although an experienced crystallographer can readily deduce the (qualitative) texture in this sample, these data present quite a challenge in reconstructing the OD for the following reasons. First, the only non-superposed pole figure is the {002}, and it is evident by examination of the whole set of data that the c-direction is aligned with the magnetic field, and therefore the {002} poles should be on the periphery of the figure where no data were taken. The implication of this is that the measured part of the {002} pole figure contains very little information about this texture, and is almost certainly normalized incorrectly because of the missing peaks. The same applies to all geometrically equivalent poles, i.e. {005} and {006} which are components of Figures 1c and 1d, respectively. We therefore have a set of data in which the only unambiguous pole figure has its major peaks missing, and another two have significant information missing also.

The data were analyzed using the method described above. The relative Bragg intensities were calculated using the crystallographic data from Cava *et al.* (1987). Twelve iterations were performed using an IBM PS2/70-386 computer running under PC-DOS. Each iteration took about 20 seconds. Figure 2 shows the calculated orientation distribution as constant v sections with ψ on the azimuth (see Kocks, 1988). As expected from the measured pole figures, the OD shows strong "fiber texture" with the *c* axis aligned with the magnetic field direction, and with no strong preferential alignment of the *a* and *b* axes.

The set of recalculated and separated pole figures is shown in Figure 3. These are in very good agreement with the measured data in Figure 1, but observe that the outer rims are now completed. It is apparent that the {002}, {005} and {006} poles have been located correctly, and that the {002} pole figure is now re-normalized (this is performed automatically by the program). The good agreement between the measured and recalculated pole figures indicates that the OD that has been determined is crystallographically consistent with the experimental data.

To demonstrate the capability of the technique described above for separating superimposed pole figures, we have taken pairs of recalculated pole figures and numerically superimposed them. Figure 4a shows the recalculated {002} pole figure which can be directly compared with Figure 1a. The difference between the two figures lies in the correct normalization of the recalculated pole figure whereas the experimental pole figure, Figure 1a, cannot be normalized because most of the intensity is at the edge. Figure 4b, however, shows the superposition of the recalculated {110} and {103} pole figures which can be compared with Figure 1b. Similarly, Figure 4c shows the superimposed {005} and {014}, cf. Figure 1c, and Figure 4d shows the superposed {006} and {200} pole figures, cf. Figure 1d. In all of these it is apparent that the OD calculation has correctly located the ⟨001⟩ directions at the top of the pole figures.

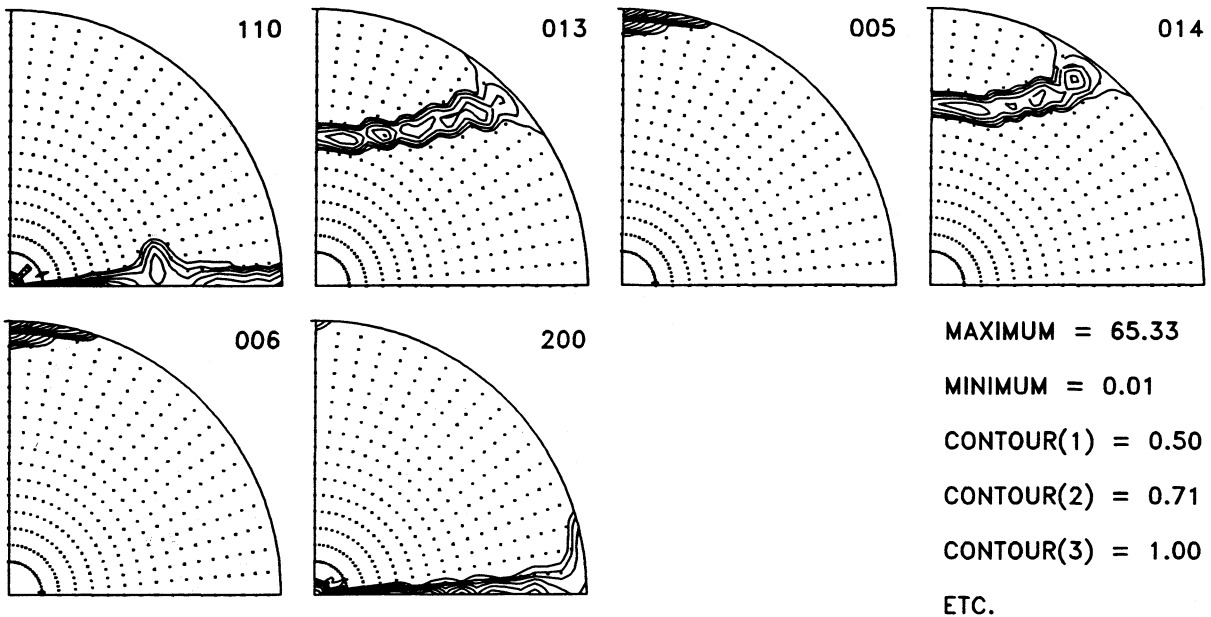

Figure 3 Recalculated pole figures from the OD shown in Figure 2, where each pole figure of the 110, 013, 005, 014, 006 and 200 reflections has been separately calculated. The indices for each pole figure are indicated at the top right of each quadrant.

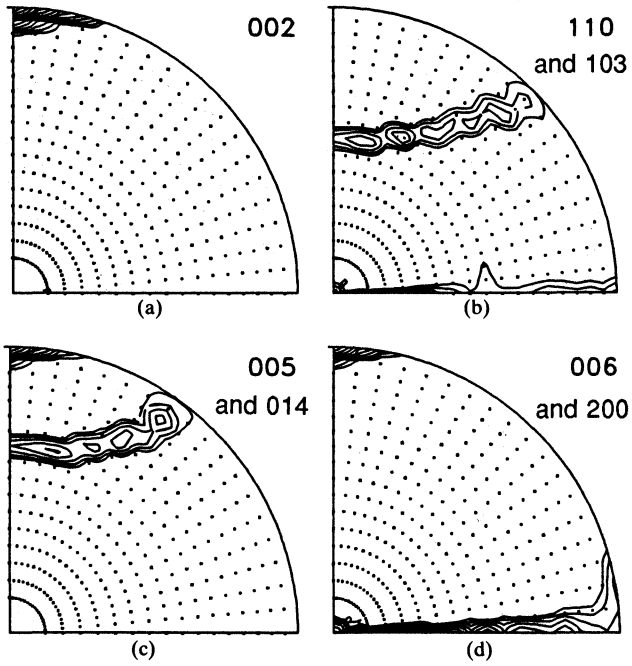

Figure 4 (a) Recalculated {002} pole figure: compare with Figure 1a. (b) Superposition of recalculated {110} and {103} pole figures: compare with Figure 1b. (c) Superposition of recalculated {005} and {014} pole figures: compare with Figure 1c. (d) Superposition of recalculated {006} and {200} pole figures: compare with Figure 1d.

3. CONCLUSIONS

We have used a modification to the WIMV algorithm to analyze the texture of a magnetically aligned superconductor powder sample. Using only four incomplete pole figures (of which three contained superposed forms) we derived an orientation distribution which shows good agreement with the experimental data. The orientation distribution shows a strong *c*-axis fiber texture, with the *c*-axes aligned in the direction of the applied magnetic field and no preferred alignment

of the *a* and *b* axes. Using this procedure we achieved a satisfactory separation of the superimposed peaks in the measured pole figures.

The present texture analysis technique can be used to study the dependence of J_c on texture in superconducting perovskites. We should note, however, that the OD does not provide information on the morphology of the grains in the polycrystalline sample, i.e., "fiber texture" samples with different grain morphologies may have similar ODs. Thus, for the study of the dependence of J_c on texture, the OD information must be complemented with direct observation of grain morphology.

4. ACKNOWLEDGEMENTS

This work was supported by the U.S. Department of Energy, Office of Basic Energy Sciences. J. S. Kallend thanks the hospitality of the Center for Materials Science, Los Alamos National Laboratory.

References

Baker, D. W. and Wenk, H.-R. (1972), *J. Geol.* **80,** 81–105.
Bunge, H.-J. (1965), *Z. Metall.*, **56,** 872–874.
Bunge, H.-J. (1982), *Texture Analysis in Materials Science,* p 62, Butterworths, London.
Cava, R. J., Batlogg, B., Chen, C. H., Rietman, E. A., Zahurak, S. M. and Werder, D. (1987), *Phys. Rev. B.*, **36,** 5719.
Emerson & Cuming Inc., Woburn, MA 01888, USA.
Hein, M., Müller, G., Piel, H., Ponto, L., Becks, M., Klein, U. and Peinige, R. M. (1989), *Appl. Phys.*, **66,** 5940.
Jin, S., Tiefel, T. H., Sherwood, R. C., Davis, M. E., van Dover, R. B., Kammlott, G. W., Fastnacht, R. A. and Keith, H. D. (1988), *Appl. Phys. Lett.*, **52,** 2074.
Kallend, J. S., Wenk, H.-R. and Heidelbach, F. (1990), Quartz Mylonite Textures: application of WIMV algorithm (unpublished research).
Kocks, U. F. (1988), *Proc. ICOTOM-8,* edited by J. S. Kallend and G. Gottstein, pp. 31–36, TMS-AIME, Warrendale, PA.
Matthies, S. and Vinel, G. W. (1982), *Phys. Stat. Sol. (b),* **112,** K111-K120.
Rollett, A. D. (1989) (unpublished research).
Salama, K., Selvamanickam, V., Gao, L. and Sun, K. (1989), *Appl. Phys. Lett.*, **54,** 2353.